Atmos. Chem. Phys. Discuss., 12, 6331–6361, 2012
www.atmos-chem-phys-discuss.net/12/6331/2012/
doi:10.5194/acpd-12-6331-2012

Atmospheric Chemistry and Physics Discussions

Ozone pollution over the Arabian Gulf – role of meteorological conditions

L. Smoydzin[1], M. Fnais[2], and J. Lelieveld[1,2,3]

[1]Max-Planck-Institute for Chemistry, Department of Atmospheric Chemistry, P.O. Box 3060, 55020 Mainz, Germany
[2]King Saud University, Riyadh, Saudi Arabia
[3]The Cyprus Institute, Centre for Energy, Environment and Water Research, Nicosia, Cyprus

Received: 31 January 2012 – Accepted: 18 February 2012 – Published: 29 February 2012

Correspondence to: L. Smoydzin (linda.smoydzin@mpic.de)

Published by Copernicus Publications on behalf of the European Geosciences Union.

Abstract

The Middle East and particularly the Arabian Gulf region are characterised by highly favourable conditions for O_3 formation in summer. We investigated the role of meteorological conditions in O_3 formation using the WRF-chem model. The dispersion of air pollutants strongly depends on local wind patterns, in particular the persistent low-level north-westerly flow known as the summer Shamal, and recurrent land-sea breeze circulation systems.

A general finding from our simulations is that extreme pollution events, with O_3 mixing ratios exceeding 150 nmol mol^{-1}, can occur regularly over the Arabian Gulf, however, their location and magnitude can vary widely. O_3 mixing ratios are highest when the outflow of the regions with major anthropogenic emissions along the coast is advected over the Gulf, where pollution plumes are captured in the shallow and stable marine boundary layer allowing little ventilation. The sea-breeze circulation often causes onshore advection of the pollution in the afternoon, affecting the densely populated coastal regions along the western shoreline of the Gulf.

When the pollution is transported deeper over land, O_3 mixing ratios are generally lower due to rapid dilution of precursor gases in the very deep convective boundary layer over the desert.

1 Introduction

Enhanced levels of ozone (O_3) pollution can be a major problem by degrading air quality in (sub)urban and industrial areas, especially in summer when its photochemical formation by the oxidation of volatile organic compounds (VOC) and catalysed by nitrogen oxides (NO_x), is most efficient. From satellite observations it is known that NO_x ($NO+NO_2$) concentrations in the Arabian Gulf area are exceptionally high (Stavrakou et al., 2008; van der A et al., 2008; Lelieveld et al., 2009). Mean concentrations of tropospheric NO_2 columns exceed 10×10^{15} molec cm^{-2} along the northern and western

coast of the Arabian Gulf (Beirle et al., 2011). Analysis of data retrieved from the TES satellite instrument reveal that O_3 concentrations are elevated in the lower and mid troposphere over the entire Middle East (Liu et al., 2009). Model calculations indicate that the Arabian Gulf region is strongly affected by photochemical smog due to high background levels of ozone by long-distance transport, highly favourable weather conditions for ozone formation and strong local pollution emissions (Lelieveld et al., 2009)

In general, climatic conditions over the Arabian Peninsula in summer are dry and hot with temperatures regularly exceeding 35 °C (Elagib and Abdu, 2010). Along the coast of the Gulf, humidity is often high in the afternoon hours due to the land-sea-breeze circulation (Hubert et al., 1983).

A frequent and persistent weather phenomenon over the Arabian Gulf in winter as well as summer are Shamal winds (Membery, 1983; Barth, 2001; Rao et al., 2003; Shi et al., 2004). The Shamal is a low level, thermally driven northerly to northwesterly flow, regularly reaching a speed of up to 30 m s^{-1}. During the night, the Shamal often weakens near the surface but strengthens at elevated levels (300–700 m) (Rao et al., 2003; Giannakopoulou and Toumi, 2011). Shamals are the predominant cause for dust outbreaks over Iraq and northern Saudi Arabia which impact visibility, air quality and the radiation budget throughout the Arabian Gulf region.

During winter, Shamals are known to be initiated after the southeastward passage of cold fronts (Perrone, 1979; Walters and Sjoberg, 1988). In summer, the semi-permanent high pressure system over the Eastern Mediterranean, which extends into northern Saudi Arabia, and a semi-permanent low pressure system over Iran lead to a north-westerly flow over the Arabian Peninsula and the Gulf (Rao et al., 2003). Rao et al. (2003) further hypothesised that conditions under which the monsoon low over India and Pakistan extends to the lee of the Zagros mountains and the south-eastern part of the Arabian Peninsula, are favourable for the outbreak of Shamals as the east-west pressure gradient is increased. The Zagros mountains to the east of the Gulf, which can exceed 2000 m altitude, strongly contribute to the channelling of the near surface air flow. Additionally they modulate the diurnal evolution of the Shamal

through orographic flows (Giannakopoulou and Toumi, 2011). Furthermore, the land-sea-breeze can modulate the Shamal by changes in the geostrophic wind component.

Particularly in summer a sea breeze regularly develops over the Arabian Gulf, however over the northern coast landward penetration of marine air masses is rare, whereas they can be advected more than 200 km inland along the south/south-western coast (Zhu and Atkinson, 2004; Eager et al., 2008). The vertical extent of the sea breeze is difficult to determine and in summer may reach an altitude of about 1.5 km (Zhu and Atkinson, 2004; Eager et al., 2008) with a return current above the onshore flow. At night the land-sea breeze over the Gulf is associated with uplift and convergence whereas during daytime it is associated with subsidence and divergence (Zhu and Atkinson, 2004). The sea breeze is initiated rather late during the day (13:00–14:00 LT) compared to other coastal areas (Eager et al., 2008). During strong Shamal conditions the sea breeze can be fully inhibited (Zhu and Atkinson, 2004).

The boundary layer over the Gulf is often very shallow and stable (Brooks and Rogers, 2000; Atkinson and Zhu, 2005; Brooks et al., 1999) as hot and dry air masses from the surrounding deserts are advected over the cooler sea resulting in a strong temperature inversion and a very shallow stable layer. Since this near-surface layer can form within an existing, deeper boundary layer it represents an “internal” boundary layer (Garratt, 1990; Angevine, 2008). If the Shamal is not too strong, thus allowing the sea breeze to develop, the onshore advection of relatively cool air from the Gulf toward the desert may also be associated with an internal boundary layer, possibly trapping air pollution near the surface in the coastal region. Highly stable marine boundary layers similarly occur e.g. over the Gulf of Maine affecting the transport and concentrations of trace gases as observed during the International Consortium for Atmospheric Research in Transport and Transformation (ICARTT)/New England Air Quality Study (Angevine et al., 2006; Fehsenfeld et al., 2006).

The objective of this study is to assess the influence of meteorological conditions (wind regime, high temperatures in summer, humidity conditions) on O_3 formation over the Arabian Gulf region. Further, we analyse the rate of photochemical O_3 formation

in view of uncertainties in the emission inventories of anthropogenic O_3 precursor sources.

2 Case study description

For our case studies, we have selected a period of five days in mid July (14–18) in the years 2009, 2010 and 2011. In general the potential for a buildup of high concentrations of O_3 is highest in summer (Lelieveld et al., 2009). During approximately half of the total of 15 days of simulation the wind direction in the boundary layer is northerly to north-westerly which is the predominant flow in July based on climatological data. However, the initial meteorological conditions on 14 July in all three years are rather distinct (Figs. 1 and 2) thus providing the opportunity to investigate O_3 formation under different ambient conditions, particularly focusing on (i) days and regions with and without the development of land-sea breeze systems and (ii) periods with and without Shamal winds.

2.1 Synoptic conditions

2.1.1 July 2009

Following the work of Rao et al. (2003) we have selected one simulation period favourable for a persistent Shamal over the Gulf. An upper level trough was located over Turkey accompanied by a ridge to the west across the Eastern Mediterranean and a ridge to the east over western Iran. The cyclone remained very stable over Turkey during the entire simulation period and propagated only slowly eastward. The surface pressure distribution shows a significant north-south gradient over the Arabian Gulf area as the Mediterranean high was strong with a ridge extending over central Saudi Arabia (Fig. 1). Such pressure conditions typically enhance the north-westerly flow near the surface (Rao et al., 2003). Compared to 2010 and 2011, wind speeds

over the Gulf were higher (maximum up to 20 m s^{-1}). Furthermore, the temperature on the simulation days in 2009 was lower (regionally more than ≈5 °C) than in the years 2010 and 2011 (Fig. 2). The temperature differences between air masses over land and water were smaller leading to a higher boundary layer over water (compared to the years 2010 and 2011). Furthermore, meteorological conditions lead to a less efficient or inhibited sea breeze. A typical phenomenon over the Gulf is the development of a shallow inversion only a few hundred metres above the sea surface (≈950 hPa) capping a stable and moist marine boundary layer. At approximately 500 hPa a very dry subtropical subsidence inversion associated with the downward motion of the Hadley circulation is typical for most days in summer (Fig. 2) (Ackermann and Cox, 1982; Reid et al., 2008).

2.1.2 July 2010

On 14 July 2010 the 500 hPa flow over the eastern Mediterranean, Iraq and Iran was almost meridional. On 15 July a weak upper level trough formed over southern Turkey which slightly intensified in the following days while it slowly propagated north-eastward. The surface pressure chart is significantly different compared to the simulation period in 2009. A weakening of the Iranian low, with a simultaneous negative pressure tendency over central Saudi Arabia and the northern Gulf was unfavourable for the development of a Shamal (Fig. 1).

2.1.3 July 2011

On 14 July a cyclone was located over the Black Sea and propagated slowly south-eastward during the following days. Generally the surface pressure distribution was similar as during the Shamal period in 2009 with a distinctive surface low over the southern Gulf and a south-eastward penetrating Mediterranean high. However, a positive pressure tendency over central Iran, Qatar and the UAE weakened or inhibited the Shamal.

3 Model setup

The fully coupled chemistry version of the Weather Research and Forecasting model (WRF-chem) (Grell et al., 2005) version 3.3.1 was used for this study. The treatment of aerosols and aerosol-cloud interactions in WRF-chem is described in detail by Fast et al. (2006) and Chapman et al. (2009) and only a brief overview of the features most relevant in this study is given below.

Gas phase chemistry is calculated using the CBMZ mechanism (Zaveri and Peters, 1999). Direct and indirect aerosol effects are calculated in the model as described by Chapman et al. (2009). The representation of aerosol activation is based on the parametrisation by Abdul-Razzak et al. (1998) and its implementation into WRF-chem follows the description by Chapman et al. (2009) and references therein. Cloud microphysical processes are calculated using the scheme by Lin et al. (1983) with modifications in order to treat cloud drop numbers prognostically. For nests with horizontal resolutions requiring the usage of a convection parametrisation we use the scheme by Grell and Devenyi (2002). For calculating aerosol thermodynamics and microphysics the Module for Simulating Aerosol Interactions and Chemistry (MOSAIC) is used (Zaveri et al., 2008). Boundary layer physics is parametrised using the Yonsei University (YSU) PBL scheme (Hong et al., 2006).

Initial and boundary conditions for gas phase species for our simulations are derived from MATCH-MPIC (Model of Atmospheric Transport and Chemistry, von Kuhlmann et al., 2003) which is ran operationally as a global chemical weather forecasting model at the Max Planck Institute for Chemistry. Initial and boundary conditions for aerosol constituents are taken from simulations performed with the global chemistry-climate model EMAC (Pringle et al., 2010). For anthropogenic emissions we use the high resolution (0.1 × 0.1°) EDGAR-CIRCE emission inventory (Doering et al., 2009a) which has been prepared in the framework of the CIRCE Project (No. 036961) by the EDGAR group (Emission Database for Global Atmospheric Research) of the EC-Joint Research Center Ispra (Italy), Climate Change Unit and has been evaluated by Doering et al. (2009b).

The setup of our simulations comprises three nests with horizontal resolutions of 48 km, 16 km and 4 km and with a vertical resolution of 53 layers with narrowly spaced model levels in the lower troposphere. If not mentioned otherwise we refer in our analysis to the 16 km grid.

4 Results

4.1 O_3 distribution and variability

For our analysis we focus on the time of day when O_3 mixing ratios reach a maximum, i.e. at 12:00 UTC = 15:00 Local Time (Fig. 3). A general finding from our simulations encompassing a total time period of 15 days is that O_3 hot spots develop regularly over the Arabian Gulf, however the location and the intensity of the O_3 pollution can vary widely.

The boundary layer over the Gulf is shallow under all conditions, being relatively deepest for the simulation period in 2009 (≈200–400 m compared to ≈50–100 m in 2010 and 2011 around 12:00 UTC). It thus appears that the formation of O_3 hot spots over the Gulf is facilitated by the inhibition of vertical transport in regions with strong pollution emissions, so that both precursor gases and the resulting O_3 accumulate near the surface. Especially in the year 2009 the boundary layer is relatively low over the north-western part of the Gulf, which is in the region with highest VOC emissions.

On the first day (14 July, Fig. 3, first row) of the simulation period, high O_3 values are simulated during all three years over the northern Gulf region with a distinctive hot spot along the coast south of Kuwait. In 2010 and 2011 O_3 mixing ratios also exceed 80 nmol mol^{-1} further inland in the late afternoon/early evening hours (especially in the area of Dammam/Al Jubayl) when the sea breeze transports polluted air over the coastal regions. Particularly on 14, 15 and 16 July 2010 the sea breeze is strong and O_3 mixing ratios are elevated (>60 nmol mol^{-1}) up to 50–100 km west of the coast line. On 15 July 2010, the weak background flow facilitates the earlier and stronger initiation of the sea breeze (about 08:00 UTC) compared to 14 July 2010, leading to the transport

of marine air masses over the coast during almost the entire day. At 12:00 UTC (15 July 2010) O_3 mixing ratios over the Gulf are very low, however, almost everywhere along the western coast they exceed 60 nmol mol^{-1} (over land) with local maxima of more than 80 nmol mol^{-1} (around 28° N). Especially in the area of Al Jubayl O_3 mixing ratios are higher on 15 July than on 14 July because (i) the sea breeze developed earlier, (ii) the boundary layer along the coast (up to ≈40 km inland) is lower on 15 July than on 14 July, thus trapping the locally formed pollution near the surface. In contrast to 2010 and 2011, on 14 July 2009 the pollution plume remains located over the sea during the whole day because the strong Shamal winds prevent the development of a sea breeze.

On the second day of the simulation (15 July 2009, Fig. 3, second row) high levels of O_3 build up again over the western Gulf where the persistent north-westerlies transport the pollution emitted in Kuwait over the Gulf which contributes to the photochemical transformation of local emissions further South, leading to the formation of O_3 mixing ratios of more than 100 nmol mol^{-1}. As a consequence of the rare event of a sea breeze developing over the northern part of the Gulf, on 15 July 2010 the highest local mixing ratios of O_3 (≈120–150 nmol mol^{-1}) are simulated along the coast of Kuwait. In the year 2011, O_3 mixing ratios are also elevated over the northern Gulf (≈80 nmol mol^{-1}) but in contrast to most other days extreme values of 100 nmol mol^{-1} are not exceeded. The general explanation for the distinct horizontal distribution of surface O_3 on 15 July 2009, 2010 and 2011 is the changing wind direction. In 2009 the wind direction is persistently north-west, whereas it is southerly or south-easterly in 2010 during the night and in the morning. In 2011 the nighttime wind direction is also north-westerly, from Kuwait over the coastal area into northern Saudi Arabia. During the time of photochemical activity the outflow direction from Kuwait is southward over land. Mixing ratios of O_3 near the surface in that location are not as high as over the sea mainly due to the deep boundary layer (≈4.5 km in the outflow region south of Kuwait) leading to the efficient mixing and dilution of the O_3 plume. The same argument holds for the lack of O_3 hot spots over the Gulf on 16 and 17 July in 2009 and 2010.

The horizontal distribution of O_3, especially in the outflow region of Kuwait appears to be generally very similar on 16 July, (Fig. 3 third row) in 2009 and 2011 though mixing ratios are significantly higher in the latter year (≈90 nmol mol^{-1} versus ≈60 nmol mol^{-1} in 2009) while the boundary layer height is very similar in both years. However, in 2011 a stable residual layer develops in the night between 15 and 16 July leading to elevated O_3 mixing ratios exceeding 60 nmol mol^{-1} at 2000 m altitude throughout the night over north-eastern Saudi Arabia, facilitating long-distance transport from the north. When the boundary layer develops in the morning of 16 July the elevated O_3 mixing ratios from the lower free troposphere significantly contribute to the high near surface values (Fig. 4, right column).

As indicated above, the outflow of Kuwait can contribute strongly to the O_3 formation over the Arabian Gulf. On 15 July in 2011 pollution from Kuwait is transported mainly over Saudi Arabia or northward over Iraq. Despite the lacking transport of O_3 precursor gases from Kuwait (or more generally polluted coastal areas) over the sea, O_3 mixing ratios over the northern Gulf exceed 80 nmol mol^{-1} at 12:00 UTC. In contrast, on 16 July in 2009 O_3 mixing ratios over the Gulf are relatively low (≈40 nmol mol^{-1}) even though the wind regime is similar as on 15 July in 2011. From Fig. 5a we can identify the regions with high VOC emissions over the northern Gulf region. The O_3 formation rate between 10:00 and 12:00 UTC on 16 July 2009 in the circled region in Fig. 5a, b is approximately 0.5–5 pmol (mol^{-1} s) whereas it reaches values twice as high on 15 July 2011 (Fig. 5c), even though the emission strength of VOC's in the area does not differ between the two years. Nevertheless, in 2011 surface VOC mixing ratios are almost a factor of two higher in this region (200–400 nmol mol^{-1}) compared to 2009 (50–100 nmol mol^{-1}). The difference is again a consequence of the substantially lower boundary layer over the Gulf in the nights between 14 and 15 July 2011 and 15 and 16 July 2009 (≈100 m in 2011 compared to 500 m in 2009). In addition to less efficient vertical mixing on 15 July 2011, the wind speed is lower than on 16 July 2009, and the reduced venting allows the buildup of high levels of O_3 precursor gases.

In our simulations we often see a second O_3 maximum building up off the coast of the United Arab Emirates (UAE). Especially in the area of Dubai (the location with highest NO_x and VOC emissions in the UAE) a land breeze regularly develops during the night, transporting O_3 precursor gases and photochemcially produced O_3 from the previous days over the Gulf.

Interestingly, a third emission hot spot is located in the area of Dammam/Al Jubayl/Bahrain (Fig. 5a) though we rarely find very high O_3 mixing ratios (larger than 100 nmol mol^{-1}) directly related to precursor emissions from this region. Only under conditions that allow development of the nocturnal land-sea breeze, emissions from this region impact O_3 formation over the Gulf. However, these conditions (temperature gradients) are not as often fulfilled as along the UAE coast, at least in our simulation periods (e.g. 14 July 2010, 18 July 2011). Nevertheless, O_3 mixing ratios are regularly enhanced in this area with values of about 70 nmol mol^{-1}.

4.2 Chemical O_3 formation regimes

In several highly polluted regions around the globe model and field data analysis provide indications that O_3 formation is VOC limited (e.g. Song et al., 2010; Yang et al., 2011) whereas NO_x limited O_3 production is reported for cities like Tokyo (Kanaya et al., 2008) and Chicago (Lin et al., 2010) for example. In the Arabian Gulf region NO_x emissions are very high, mainly in and near the populated areas (Kuwait City, Dammam, Riyadh, Dubai) due to industry, the energy sector as well as land traffic and relatively intense ship emissions. High VOC levels are common in the atmosphere over the entire area due to emissions from oil drilling platforms in the Gulf, refineries located mainly near the coast as well as drilling fields and related industries further inland.

O_3 mixing ratios in locations for which NO_x hot spots are simulated are never extraordinary high, partly due to O_3 titration by local NO emissions, whereas they can exceed 100 nmol mol^{-1} in the outflow of the regions mentioned above. During night O_3 is almost completely depleted in these locations due to the titration by NO. Our simulations

indicate that O_3 formation is VOC limited only very close to the NO_x sources while a few kilometres downwind O_3 formation rapidly enters into a NO_x limited regime. To show the regional differences of O_3 formation regimes and compare the results with other studies, we apply the ratio of the production of hydrogen peroxide and nitric acid $P(H_2O_2)/P(HNO_3)$ as an indicator for VOC or NO_x limited O_3 formation regimes (Sillman, 1995; Tonnesen and Dennis, 2000). Song et al. (2010) find that this ratio is always below 0.14 (= VOC limited) in Mexico City and mostly exceeds 0.24 (= NO_x limited) downwind of the city with small areas where O_3 formation is in the transition regime. Figure 6 shows as an example $P(H_2O_2)/P(HNO_3)$ for 12:00 UTC on 14 July 2011. At this point in time O_3 mixing ratios exceed 100 nmol mol^{-1} along the shoreline of the northern Gulf and over the centre of the Gulf. The wind direction in the morning hours of 14 July is westerly in northern Kuwait blowing polluted air masses eastward over the Gulf. The horizontal wind in Kuwait City has a stronger southerly component leading to a second outflow plume south of Kuwait which remains over land. O_3 formation in the southern plume is still VOC limited or in the transition regime up to ≈100 km downwind of the source region whereas it quickly turns into a NO_x limited regime over the Gulf (≈30 km east of the coast). Several factors contribute to the differences in the chemical regimes of these two plumes: (i) the southern plume is blown over a region with little or no VOC emissions whereas the VOC load over the sea is much higher (due to local emissions there and to less efficient venting to higher altitudes) (ii) the southern plume is blown along the coast where the boundary layer is not as high as further inland which, on other days, leads to a more efficient(vertical) dilution of the plume (e.g. 15 July 2011, 16, 17 July 2009) and (iii) the wind speed along the coast is higher than over the northern Gulf leading to a faster removal by the southern plume by transport. Similar as in Kuwait, O_3 formation is also VOC limited downwind of Dammam, Bahrain, Dubai and Riyadh.

Our results indicate that in general O_3 formation is mainly NO_x limited during episodes of very high O_3 mixing ratios (>90 nmol mol^{-1}) with very few exceptions (Fig. 7). During the first hours of photochemical activity until ≈09:00 UTC O_3 formation

is VOC limited in more locations near the main emission sources, however only until the formation of NO_2 and HO_2 by VOC oxidation products start dominating O_3 formation over almost the entire Gulf region.

4.3 O_3 response to changing emissions

Since the simulated O_3 mixing ratios strongly depend on the emission source strength and as all state-of-the-art inventories for anthropogenic emissions are associated with substantial regional uncertainties, we performed a series of sensitivity simulations with varied emissions for NO_x and VOC for the year 2011. Additionally, these sensitivity simulations help us quantifying the impact of the pollution outflow of certain coastal cities on O_3 formation over the Gulf. Since we found that especially the outflow of Kuwait can significantly impact O_3 formation over the Gulf region, a series of sensitivity simulations focus on emission reduction scenarios for Kuwait and the impact on O_3 formation downwind of the Kuwait outflow (Table 1). We have conducted a second set of sensitivity studies with reduced emissions for the entire region around the Arabian Gulf.

Reducing both, VOC and NO_x emissions from Kuwait by 50 % results in a decrease of O_3 mixing ratios in the outflow region by up to 10–15 % on 15 July 2011 and by 15–20 % on 16 July 2011 (Fig. 8). Decreasing VOC emissions only (VOC_K), leads to an even stronger decrease of O_3 mixing ratios downwind of Kuwait by more than 30 % (15 July) and to a decrease of up to 65 nmol mol^{-1} (more than 50 %) for 16 July 2011 at times and locations of maximum O_3 (over the northern Arabian Gulf). Reducing only NO_x emissions leads to a significant increase in O_3 mixing ratios in Kuwait and downwind of the city. Over the northern Gulf, O_3 mixing ratios are decreased due to lower NO_x background levels due to reduced emissions from Kuwait.

Less efficient titration of O_3 by NO under conditions with lower NO_x emissions contributes to the increase in O_3 mixing ratios in scenarios ALL_K and NOX_K.

We discussed above that the relatively low O_3 mixing ratios on 15 July 2011 can be explained by the changing wind directions compared to 16 July, transporting polluted

air masses from the Kuwait area south over land. Indeed we hardly see any differences in O_3 mixing ratios from the emission reduction scenarios compared to our base simulation over the northern Gulf on 15 July (Δ $O_3 \approx 2$ nmol mol^{-1}). However, mixing ratios in the outflow of Kuwait decrease significantly on 16 July 2011 in scenarios NOX_K, VOC_K and ALL_K.

When decreasing anthropogenic emissions in the entire region around the Arabian Gulf, scenario NOX_A leads to the strongest reduction in O_3 concentrations. Nevertheless, O_3 mixing ratios would still exceed strongly European and American air quality standards, though for a shorter time period.

5 Discussion

Our analysis of the O_3 build-up over the Arabian Gulf region indicates that meteorological conditions to a large degree control the strength of pollution events. The formation of thermal internal boundary layers over the Gulf and in coastal regions can strongly reduce vertical mixing and dilution of the emissions caused by traffic and industry, effectively trapping the air pollution near the surface. Near-surface boundary layer heights over the Gulf often do not exceed a few hundred meters. Further, the strength of the Shamal wind plays an important role, not only directly through the south-easterly transport of pollution plumes, but also indirectly by its regulatory role of sea breeze circulations. In turn, the strength of the Shamal is modulated by the pressure gradient between the eastern Mediterranean ridge and the Persian trough, the latter being an extension of the South Asian monsoon over the Arabian Sea. When the Shamal is strong the sea breezes can be suppressed, whereas in the reverse case, at wind speeds of a few meters per second or less, they typically develop in the afternoon. The sea breeze circulations transport relatively cool and moist surface air over land, and the temperature inversion between these marine air masses and the hot desert air aloft prevents vertical mixing from the internal boundary layer. Again this traps pollution near the surface, though not as efficient as in the very shallow boundary layer

over the Gulf. Deeper inland, sometimes up to 100 kilometres from the coast, the dry convection over the desert erodes the inversion, leading to efficient vertical mixing up to 5 kilometres altitude. It was hypothesised by Lelieveld et al. (2009) and indicated in the studies by Li et al. (2001) and Liu et al. (2009) that the region is strongly influenced by long-range transport of air pollution, with the possible consequence that it is difficult to reduce O_3 mixing ratios over the Gulf by applying more strict local emission controls. Measurements of aerosol concentrations and back-trajectory calculations, conducted during the United Arab Emirates Unified Aerosol Experiment, also indicate that long-range transport of aerosols from eastern Europe and Africa contribute to the local particulate mass (Reid et al., 2008). Even though our present study does not focus on the contribution by long-range transport, we find that it is largely limited to the boundary layer. During one occasion (15–16 July 2011) it appears that long-range transport of O_3 enriched air contributed to enhanced O_3 mixing ratios in a night-time residual boundary layer (~2 km altitude). After a deep convective boundary layer developed over the desert, the pollution was mixed to the surface. We also analysed the contribution of large-scale subsidence of O_3 rich mid-tropospheric air into the boundary layer, and do not find substantial effects on boundary layer O_3 mixing ratios. The largest contribution of large-scale subsidence (1–4 nmol mol^{-1}) is found over coastal areas in the late afternoon and early evening hours where subsidence is strong and the boundary layer can still reach altitudes of 1–3 km. Although these subsiding O_3-rich air masses pre-condition the photochemical regime, the development of extreme pollution events in summer, with near-surface O_3 levels exceeding 100 nmol mol^{-1}, are largely attributed to local emissions.

The study by Lelieveld et al. (2009), using a global chemistry-climate model (EMAC), suggests that O_3 mixing ratios generally exceed European air quality standards (~55 nmol mol^{-1} during 8 h) in summer over large areas. The present study, which provides greater detail by the simulation of small-scale meteorological conditions, shows that even though average O_3 mixing ratios are typically high along the western Gulf coast, episodes of very high ozone alternate with periods of moderate O_3 levels

(<55 nmol mol^{-1}). The course grid resolution of EMAC (~100 km) is insufficient to resolve the sea breeze circulation systems, although the Shamal and the boundary layer height over the Gulf are reasonably well represented. For locations deeper inland, for example in Riyadh, being a city with very high NO_x emissions (Beirle et al., 2011), our present simulations show enhanced O_3 mixing ratios (>55 nmol mol^{-1}) mostly in events during which pollution plumes are advected from Kuwait or the Bahrain/Dammam/Al Jubayl area, as the local emissions in Riyadh rather titrate O_3, leading to high NO_2 mixing ratios. Due to the high boundary layer over the desert (up to 5 km) the locally emitted pollutants are efficiently mixed and diluted throughout the lower atmosphere.

With a horizontal model resolution of 16 km, as used for most of our current analysis, we may nevertheless underestimate local O_3 mixing ratios due to resolution limitations (Tie et al., 2010). Indeed, in the 4 km resolution domain O_3 mixing ratios over the Gulf can even exceed 200 nmol mol^{-1} on 14 July 2010, and on 14 and 16 July 2011. However, the spatial patterns of O_3 are very similar compared to the 16 km horizontal resolution version of the model, indicating that Shamal winds and sea breezes are represented realistically.

For a more accurate quantification of O_3 mixing ratios in the region the major issue is probably the limited knowledge of NO_x and VOC emissions in and around the Arabian Gulf region, whilst the present study relies on a global emission dataset (Doering et al., 2009a,b). There is also a need to improve the knowledge of the speciation of VOCs emitted in the region since the O_3 production potential among various VOCs can differ substantially (Butler et al., 2011). Finally, we recommend that measurements are performed and made available to test and improve model results.

6 Conclusions

We investigated the role of meteorological conditions in the build-up of O_3 over the Arabian Gulf, including severe O_3 pollution events. Episodes with O_3 mixing ratios

exceeding 150 nmol mol^{-1} appear to occur regularly, however, the location and the magnitude of such events can vary widely. Important factors include the northwesterly Shamal winds and sea breeze circulation systems. Mixing ratios of O_3 are highest in the outflow from regions with major anthropogenic emissions along the coast, typically when the air is advected over the sea where the pollution plume is captured in the very shallow and stable marine boundary layer allowing little ventilation. The emissions of O_3 precursor gases from oil drilling platforms, trans-shipment activities and exhausts from ship traffic enhance the O_3 production potential over the sea. However, without the transport of NO_x and VOC rich air masses from the coastal region, polluted by road transport, energy production and petrochemical industries, these offshore emissions would only moderately enhance the formation of O_3 (~60 nmol mol^{-1}), and not lead to mixing ratios in excess of 100 nmol mol^{-1}. Though we simulate maximum O_3 mixing ratios over the Arabian Gulf, the onshore advection in sea breeze circulations affects the coastal region along the western shores, being most densely populated. In cases of advection of pollution plumes over land rather than over the sea, O_3 mixing ratios are generally lower due to the more efficient mixing and dilution of O_3 and precursor gases in the very deep convective boundary layers over the desert. Our analysis of O_3 production regimes reveals that O_3 formation is only VOC limited in urban regions with high NO_x emissions such as Kuwait, Bahrain, Dubai and Riyadh. Downwind of these cities and in most of the Arabian Gulf region the O_3 formation is NO_x limited.

Acknowledgements. The research leading to these results has received funding from the King Saud University, Riyadh. The research leading to these results has also received funding from the European Research Council under the European Union's Seventh Framework Programme (FP7/2007-2013)/ERC grant agreement no. 226144. We thank Patrick Jöckel for providing access to EMAC data.

The service charges for this open access publication have been covered by the Max Planck Society.

References

Abdul-Razzak, H., Ghan, S., and Rivera-Carpio, C.: A parameterization of aerosol activation 1. Single aerosol type, J. Geophys. Res., 103, 6123–6131, 1998. 6337

Ackermann, S. and Cox, S.: The Saudi Arabian heat Low: Aerosol Distributions and Thermodynamic Structure, J. Geophys. Res., 87, 8991–9002, 1982. 6336

Angevine, W.: Transitional, entraining, cloudy, and coastal boundary layers, Acta Geophysica, 56, 2–20, doi:10.2478/s11600-007-0035-1, 2008. 6334

Angevine, W., Hare, J., Fairall, C., Wolfe, D., Hill, R., Brewer, W., and White, A.: Structure and formation of the highly stable marine boundary layer over the Gulf of Maine, J. Geophys. Res., 111, D23S22, doi:10.1029/2006JD007465, 2006. 6334

Atkinson, B. and Zhu, M.: Radar-duct boundary-layer characteristics over the area of The Gulf, Q. J. Roy. Meteorol. Soc., 131, 1923–1953, 2005. 6334

Barth, H.-J.: Characteristics of the wind regime north of Jubail, Saudi Arabia, based on high resolution wind data, J. Arid Environ., 47, 387–402, 2001. 6333

Beirle, S., Boersma, K., Platt, U., Lawrence, M., and Wagner, T.: Megacity Emissions and Lifetimes of Nitrogen Oxidees Probed from Space, Science, 333, 1737–1739, 2011. 6333, 6346

Brooks, I. and Rogers, D.: Aircraft observations of the mean and turbulent structure of a shallow boundary layer over the Persian Gulf, Bound. Lay. Meteorol., 95, 189–210, 2000. 6334

Brooks, I., Goroch, A., and Rogers, D.: Observations of Strong Surface Radar Ducts over the Persian Gulf, J. Appl. Met., 38, 1293–1310, 1999. 6334

Butler, T., Lawrence, M., Taraborrelli, D., and Lelieveld, J.: Multi-day ozone production potential of volatile organic compounds calculated with a tagging approach, Atmos. Environ., 45, 4082–4090, 2011. 6346

Chapman, E. G., Gustafson Jr., W. I., Easter, R. C., Barnard, J. C., Ghan, S. J., Pekour, M. S., and Fast, J. D.: Coupling aerosol-cloud-radiative processes in the WRF-Chem model: Investigating the radiative impact of elevated point sources, Atmos. Chem. Phys., 9, 945–964, doi:10.5194/acp-9-945-2009, 2009. 6337

Doering, U., Monni, S., Pagliari, V., Orlandini, L., van Aardenne, J., and SanMartin, F.: CIRCE report D8.1.1 - Emission inventory for the past period 1990–2005 on 0.1×0.1 grid, Tech. rep., Project FP6: 6.3, No. 036961, 2009a. 6337, 6346

Doering, U., van Aardenne, J., Monni, S., Pagliaria, V., Orlandini, L., and SanMartin, F.: CIRCE

report D8.1.3 – Update of gridded emission inventories, addition of period 1990-2005 and the years 2010, 1015, 2050, Tech. rep., Project FP6: 6.3, No. 036961, 2009b. 6337, 6346
Eager, R., Raman, S., Wootten, A., Westphal, D., Reid, J., and Mandoos, A. A.: A climatological study of the sea and land breezes in the Arabian Gulf region, J. Geophys. Res., 113, D15106, doi:10.1029/2007JD009710, 2008. 6334
Elagib, N. and Abdu, A. A.: Development of temperatures in the Kingdom of Bahrain from 1947 to 2005, Theor. Appl. Climatol., 101, 269–279, doi:10.1007/s00704-009-0205-y, 2010. 6333
Fast, J., Gustafson Jr, W., Easter, R., Zaveri, R., Barnard, J., Chapman, E., Grell, G., and Peckham, S.: Evolution of ozone, particulates, and aerosol direct radiative forcing in the vicinity of Houston using a fully coupled meteorology-chemistry-aerosol model, J. Geophys. Res., 111, D21305, doi:10.1029/2005JD006721, 2006. 6337
Fehsenfeld, F. C., Ancellet, G., Bates, T. S., Goldstein, A. H., Hardesty, R. M., Honrath, R., Law, K. S., Lewis, A. C., Leaitch, R., McKeen, S., Meagher, J., Parrish, D. D., Pszenny, A. A. P., Russell, P. B., Schlager, H., Seinfeld, J., Talbot, R., and Zbinden, R.: International Consortium for Atmospheric Research on Transport and Transformation (ICARTT): North America to EuropeOverview of the 2004 summer field study, J. Geophys. Res., 111, D23S01, doi:10.1029/2006JD007829, 2006. 6334
Garratt, J.: The internal boundary layer – a reveiw, Bound. Lay. Meteorol., 50, 171–203, 1990. 6334
Giannakopoulou, E. and Toumi, R.: The Persian Gulf summerime low-level jet over sloping terrain, Q. J. Roy. Meteorol. Soc., 138, 145–157, doi:10.1002/qj.901, 2011. 6333, 6334
Grell, G. and Devenyi, D.: A generalized approach to parameterize convection combining ensemble and data assimilation techiques, Geophys. Res. Lett., 29, 1693, 1693, doi:10.1029/2002GL015311, 2002. 6337
Grell, G., Peckham, S., Schmitz, R., McKeen, S., Frost, G., Skamarock, W., and Eder, B.: Fully coupled 'online' chemistry within the WRF model, Atmos. Environ., 39, 6957–6975, 2005. 6337
Hong, S., Noh, Y., and Dudhia, J.: A new vertical diffusion package with an explicit treatment of entrainment processes, Mon. Weather Rev., 134, 2318–2341, 2006. 6337
Hubert, W., Hull, A., Morford, D., and Englebretson, R.: Forecasters handbook for the Middle East/Arabian Sea, Naval Environ. Predict. Res. Facil., Monterey, Calif., 1983. 6333
Kanaya, Y., Fukuda, M., Akimoto, H., Takegawa, N., Komazaki, Y., Yokouchi, Y., Koike, M., and Kondo, Y.: Urban photochemistry in central tokyo: 2. Rates and regimes of oxidant (O_3+NO_2)

production, J. Geophys. Res., 113, D06301, doi:10.1029/2007JD008671, 2008. 6341
Lelieveld, J., Hoor, P., Jöckel, P., Pozzer, A., Hadjinicolaou, P., Cammas, J.-P., and Beirle, S.: Severe ozone air pollution in the Persian Gulf region, Atmos. Chem. Phys., 9, 1393–1406, doi:10.5194/acp-9-1393-2009, 2009. 6332, 6333, 6335, 6345
Li, Q., Jacob, D., Logan, J., Bey, I., r.M. Yantosca, Liu, H., Martin, R., Fiore, A., Field, B., and Duncan, B.: A Tropospheric Ozone Maximum Over the Middle East, Geophys. Res. Lett., 28, 3235–3238, 2001. 6345
Lin, J.-T., Wuebbles, J., Huang, H.-C., Tao, Z., Caughey, M., Liang, X.-Z., Zhu, J.-H., and Holloway, T.: Potential effects of climate and emission changes on surface ozone in the Chicago area, J. Great Lakes Res., 36, 59–64, doi:10.1016/j.jglr.2009.09.004, 2010. 6341
Lin, Y.-L., Farley, R., and Orville, H.: Bulk Parameterization of the Snow Field in a Cloud Model, J. Climate Appl. Met., 22, 1065–1092, 1983. 6337
Liu, J., Jones, D., Worden, J., Noone, D., Parrington, M., and Kar, J.: Analysis of the summertime buildup of tropospheric ozone abundances over the Middle East and North Africa as observed by the Tropospheric Emission Spectrometer instrument, J. Geophys. Res., 114, D05304, doi:10.1029/2008JD010993, 2009. 6333, 6345
Membery, D. A.: Low level wind profiles during the Gulf shamal, Weather, 38, 18–24, 1983. 6333
Perrone, T.: Winter shamal in the Persian Gulf, Technical Report TR-70-06, Naval Environmental Prediction Research Facility, Monterey, USA, 1979. 6333
Pringle, K. J., Tost, H., Message, S., Steil, B., Giannadaki, D., Nenes, A., Fountoukis, C., Stier, P., Vignati, E., and Lelieveld, J.: Description and evaluation of GMXe: a new aerosol submodel for global simulations (v1), Geosci. Model Dev., 3, 391–412, doi:10.5194/gmd-3-391-2010, 2010. 6337
Rao, P., Hatwar, H., Al-Sulaiti, M., and Al-Mulla, A.: Summer shamals over the Arabian Gulf, Weather, 58, 471–478, 2003. 6333, 6335
Reid, J., Piketh, S., Walker, A., Burger, R., Ross, K., Westphal, D., Bruintjes, R., Holben, B., Hsu, C., Jensen, T., Kahn, R., Kuciauskas, A., Mandoos, A. A., Mangoosh, A. A., Miller, S., Porter, J., Reid, E., and Tsay, S.-C.: An overview of IAE flight operations: Observations of summertime atmospheric thermodynamic ana aerosol profiles of the southern Arabian Gulf, J. Geophys. Res., 113, D14213, doi:10.1029/2007JD009435, 2008. 6336
Shi, J., Chang, S., Holg, T., Hogan, T., and Westphal, D.: A Meteorological Reanalysis for the 1991 Gulf War, Mon. Weather Rev., 132, 623–640, 2004. 6333

Sillman, S.: The use of NO_y, H_2O_2, and HNO_3 as indicator for ozone-NO_x-hydrocarbon sensitivity in urban locations, J. Geophys. Res., 100, 14175–14188, 1995. 6342

Song, J., Lei, W., Bei, N., Zavala, M., de Foy, B., Volkamer, R., Cardenas, B., Zheng, J., Zhang, R., and Molina, L. T.: Ozone response to emission changes: a modeling study during the MCMA-2006/MILAGRO Campaign, Atmos. Chem. Phys., 10, 3827–3846, doi:10.5194/acp-10-3827-2010, 2010. 6341, 6342

Stavrakou, T., Müller, J.-F., Boersma, K., Smedt, I. D., and van der A, R.: Assessing the distribution and growth rates of NO_x emission sources by inverting a 10-year record of NO_2 columns, Geophys. Res. Lett., 35, L10801, doi:10.1029/2008GL033521, 2008. 6332

Tie, X., Brasseur, G., and Ying, Z.: Impact of model resolution on chemical ozone formation in Mexico City: application of the WRF-Chem model, Atmos. Chem. Phys., 10, 8983–8995, doi:10.5194/acp-10-8983-2010, 2010. 6346

Tonnesen, G. S. and Dennis, R.: Analysis of radical propagation efficiency to assess ozone sensitivity to hydrocarbons and NO_x 1. Local indicators of instantaneous odd oxygen production sensitivity, J. Geophys. Res., 105, 9213–9225, 2000. 6342

van der A, R., Eskes, H., Boersma, K., van Noije, T., van Roozendaal, M., de Smedt, I., Peters, D., and Meijer, E.: Trends, seasonal variability and dominant NO_x sources derived from a ten year record of NO_2 measured from space, J. Geophys. Res., 113, D04302, doi:10.1029/2007JD009021, 2008. 6332

von Kuhlmann, R., Lawrence, M., Crutzen, P., and Rasch, P.: A model for studies of tropospheric ozone and nonmethane hydrocarbons: Model description and ozone results, J. Geophys. Res., 108, 4294, doi:10.1029/2002JD002893, 2003. 6337

Walters, K. and Sjoberg, W.: The persian gulf region – A climatological study, USAFETAC TN-88/002, USAF Environmental Technical application Center, Scott Air Force Base, IL, 62 pp., available from USAF Environmental Technical Application Center, Scott Air Force Base, IL62225, 1988. 6333

Yang, Q., Wang, Y., Zhao, C., Liu, Z., GustafsonJr., W. I., and Shao, M.: NO_x Emission Recuction and its Effects on Ozone during the 2008 Olympic Games, Environ. Sci. Technol., 45, 6406–6410, 2011. 6341

Zaveri, R. and Peters, L.: A new lumped structure photochemical mechanism for large-scale applications, J. Geophys. Res., 104, 30387–30415, 1999. 6337

Zaveri, R., Easter, R., Fast, J., and Peters, L.: Model for Simulating Aerosol Interactions and Chemistry (MOSAIC), J. Geophys. Res., 113, D13204, doi:10.1029/2007JD008782, 2008.

6337

Zhu, M. and Atkinson, B.: Observed and modlelled climatology of the land-sea breeze circulation over the Persian Gulf, Int. J. Climatol., 24, 883–905, 2004. 6334

Table 1. Overview of simulated scenarios with reduced anthropogenic emissions.

ALL_K	NO_x, VOC reduced by 50 % for Kuwait region
NOX_K	NO_x reduced by 50 % for Kuwait region
VOC_K	VOC reduced by 50 % for Kuwait region
ALL_A	NO_x, VOC increased by 50 % for the Gulf region
NOX_A	NO_x increased by 50 % for the Gulf region
VOC_A	VOC increased by 50 % for the Gulf region

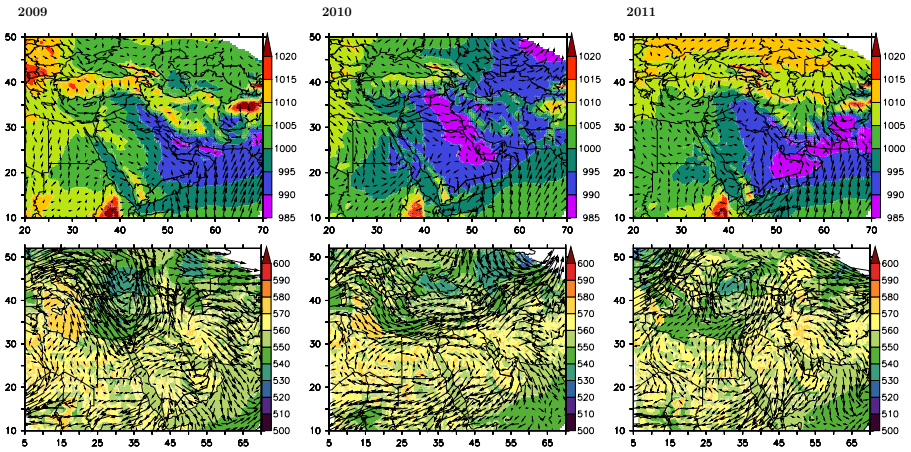

Fig. 1. Sea-level pressure (hPa) at the surface (upper row) and geopotential (gpm) at 500 hPa (lower row) at 12:00 UTC, 14 July 2009, 2010 and 2011 (48-km domain).

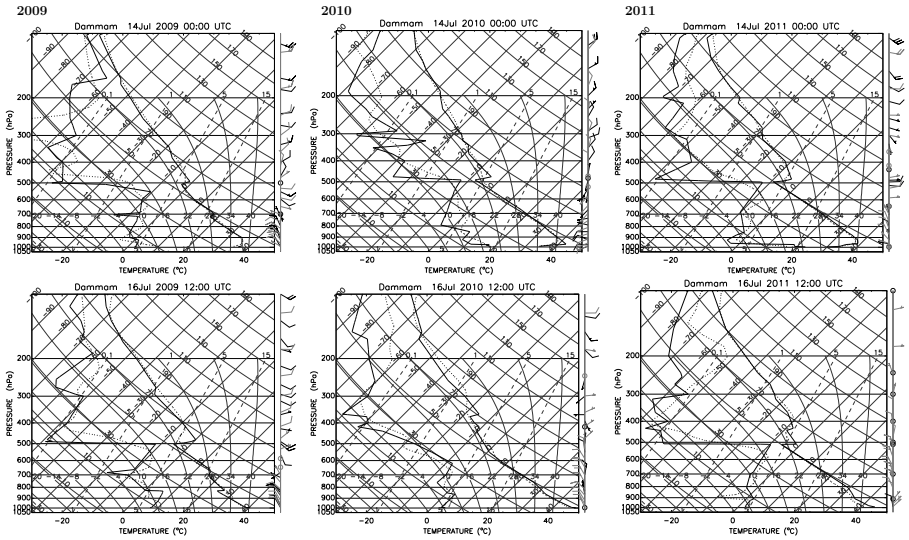

Fig. 2. Skew-log-T diagrams for Dammam at 00:00, 14 July and 12:00 UTC, 16 July. Dotted: WRF-chem, solid line: sonde measurements (University of Wyoming, http://weather.uwyo.edu/upperair/sounding.html).

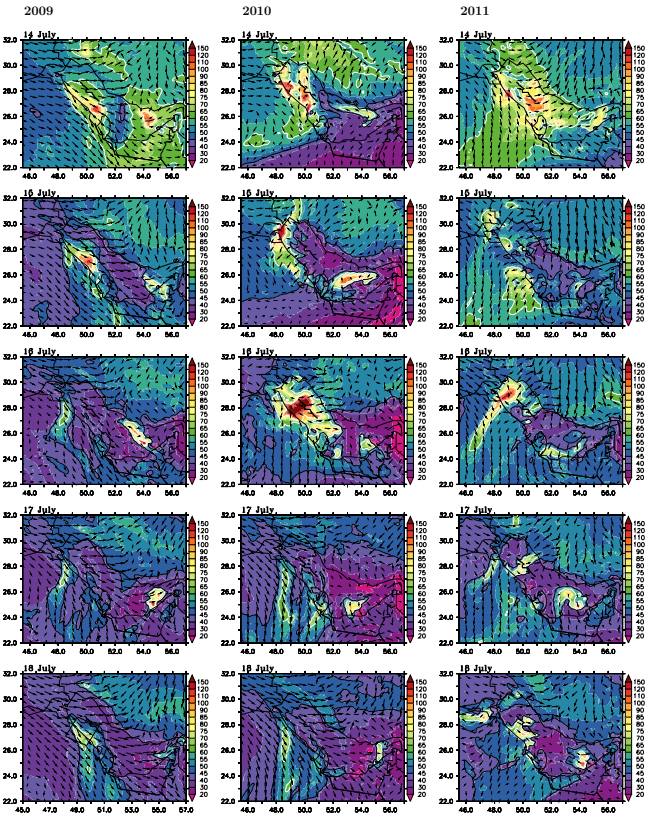

Fig. 3. Surface O_3 mixing ratios at 12:00 UTC on 14–18 July 2009 (left column), 2010 (middle column) and 2011 (right column).

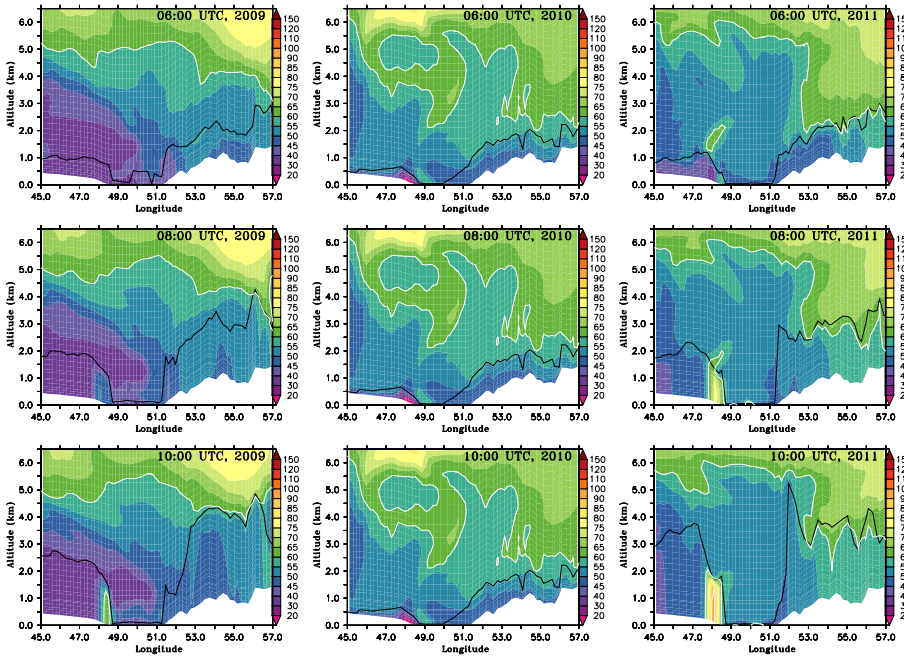

Fig. 4. Cross section along 28° N showing O_3 mixing ratios at 06:00, 08:00 and 10:00 UTC, 16 July. The black lines indicate the boundary layer height.

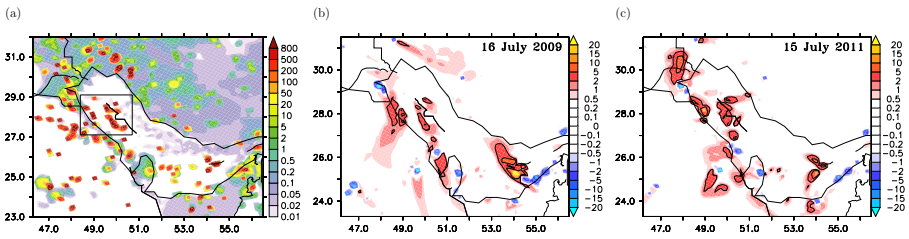

Fig. 5. Total VOC emissions (nmol mol^{-1}) in the lowest model layer **(a)**. Net O_3 production (nmol/(mol^{-1} h)) in the lowest model level at 12:00 UTC on 16 July 2009 **(b)** and 15 July 2011 **(c)**.

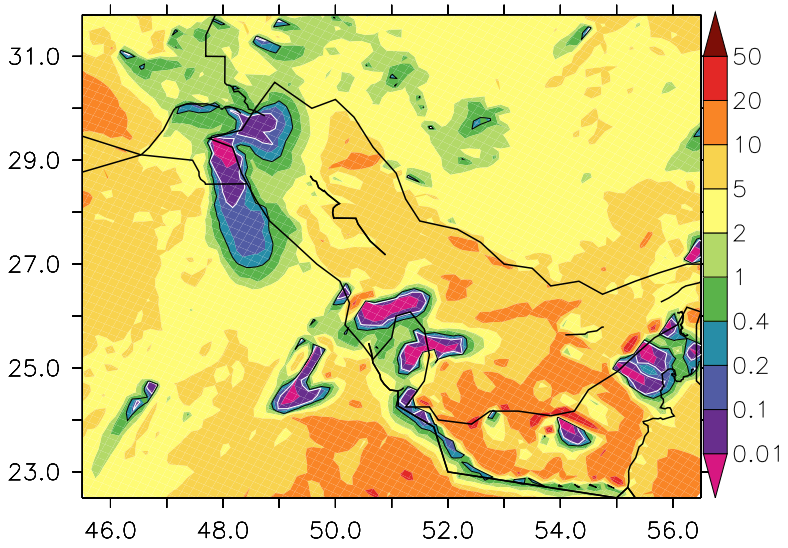

Fig. 6. $P(H_2O_2)/P(HNO_3)$ at 12:00 UTC on 14 July 2011 at the surface.

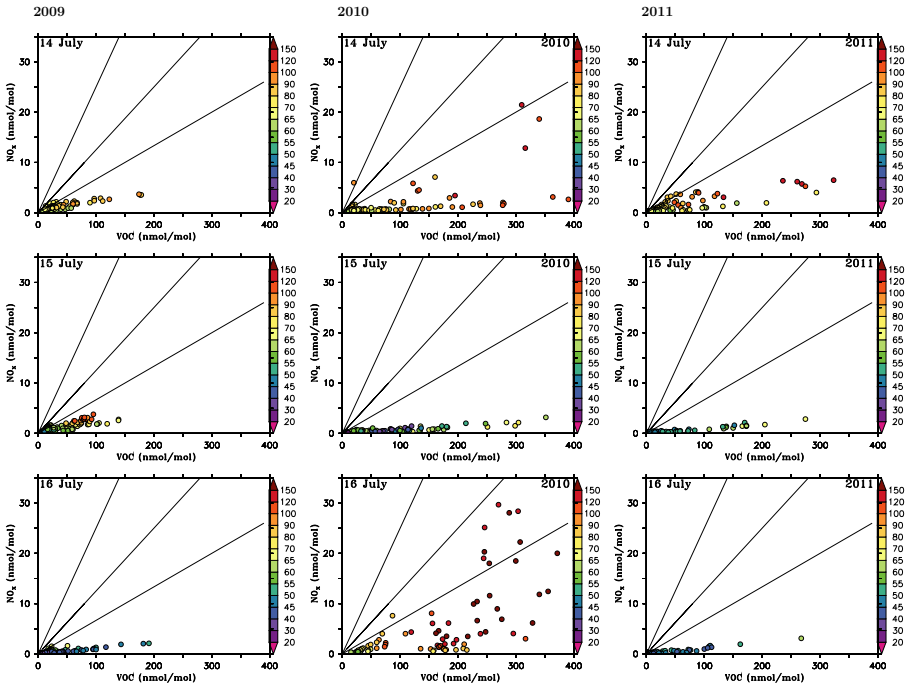

Fig. 7. Surface O_3 mixing ratios for all grid points within the coastal area of the northern Gulf (see marked area in Fig. 3, 18 July 2009), 12:00 UTC, 14–16 July 2009 (left column), 2010 (middle column) and 2011 (right column). Lines in the plots indicate the 4:1, 8:1 and 15:1 ratios between VOC's and NO_x. The colour bar shows O_3 mixing ratios (nmol mol^{-1}).

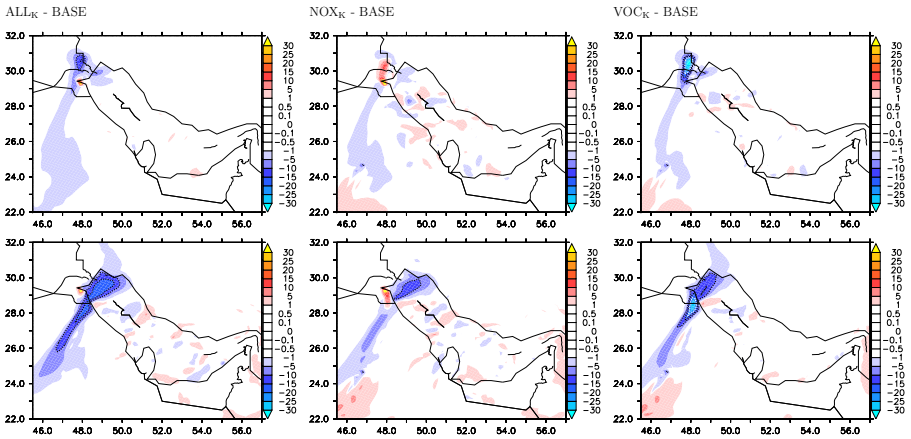

Fig. 8. Relative difference in surface O_3 mixing ratios (%) between scenarios with different emissions for Kuwait at 12:00 UTC, 15 July 2011 (upper row) and 12:00 UTC 16 July 2011 (lower row). The emission scenarios are listed in Table 1.